Int. J. Heat Mass Transfer. Vol. 13, pp. 997–1011. Pergamon Press 1970. Printed in Great Britain

DIRECT CONTACT HEAT TRANSFER WITH CHANGE OF PHASE: BUBBLE CONDENSATION IN IMMISCIBLE LIQUIDS

J. ISENBERG
Faculty of Mechanical Engineering

and

S. SIDEMAN
Faculty of Chemical Engineering
Technion—Israel Institute of Technology, Haifa, Israel

(*Received* 5 *August* 1969 *and in revised form* 4 *November* 1969)

Abstract—Bubble condensation in immiscible liquids is associated with the development of 3-phase heat exchangers applicable for heat recovery at low driving forces.

Single bubbles of volatile organic fluids cooling under heat transfer controlled conditions while rising freely in water and aqueous-glycerol solutions, were studied experimentally and theoretically. Unlike condensation in single component systems the two-component, 3-phase system is characterized by condensate accumulation within the confines of the collapsing bubble, which greatly hinders interfacial mobility. A finite difference solution in the laminar flow field was achieved by modifying the potential flow field to yield convective terms equivalent to the laminar terms in the energy equation. The presence of non-condensables is also accounted for. The agreement with experiment is very good, particularly at low Jakob Number.

NOMENCLATURE

A, area;
c_p, specific heat;
G, ratio, liquid to vapor density within the bubble, ρ_L/ρ_v;
h, heat-transfer coefficient, instantaneous;
J, dimensionless velocity function, $(u_s^2 + w_s^2)/w_\infty^2$;
k, thermal conductivity;
k_V, velocity factor for modified potential flow;
L, latent heat;
p, pressure;
q, rate of heat transfer;
R, bubble radius;
$\dot{R}$, velocity of bubble wall;
$\hat{R}$, specific gas constant;
r, radius;
T, temperature;
T^*, saturation temperature corresponding to p^*;
t, time;
u, velocity component;
V, volume;
w, velocity component;
w_∞, velocity of rise, approach velocity of continuous medium;
w_∞^*, system velocity of rise corresponding to $\beta^3 = 0{\cdot}5$;
y, dimensionless radius;
z, axisymmetric cylindrical coordinate, directed along axis of symmetry.

Greek symbols

α, thermal diffusivity;

β, dimensionless bubble radius;
$\dot{\beta}$, dimensionless velocity of bubble wall, $d\beta/d\tau$;
Γ, initial mole fraction of noncondensables;
θ, dimensionless temperature, $(T - T_\infty)/(T^* - T_\infty)$;
θ, polar angle;
μ, transformed polar angle, $\cos\theta$;
ρ, density;
τ, dimensionless time, Fourier number, $\alpha t/R_0^2$;
$\hat{\tau}$, dimensionless time appropriate for bubble collapse with translatory motion, $Pe^{*\frac{1}{2}}\,Ja\,\tau$;
Φ, dimensionless velocity potential;
ϕ, velocity potential;
Ψ, dimensionless stream function;
ψ, stream function;
ω, axisymmetric cylindrical coordinate, radially directed.

Subscripts

B, point of boundary-layer separation;
c, cavitational flow;
f, final;
g, noncondensables;
L, liquid;
o, initial;
s, rectilinear flow around a sphere of constant diameter;
T, total;
v, vapor;
w, wall;
∞, infinity.

Superscripts

$*$, system.

Dimensionless groups

Ja, Jakob number $(\rho c_p \Delta T/\rho_v^* L)$;
Nu, Nusselt number $(h2R/k)$;
Pe, Péclét number $(w_\infty 2R_o/\alpha)$;
Pe^*, system Péclét number $(w_\infty^* 2R_o/\alpha)$;
Pr, Prandtl number $(\mu c_p/k)$.

INTRODUCTION

DIRECT contact heat transfer with change of phase provides the advantage of smaller flow rates of the transfer fluid, convenient separation of the fluids, and very high heat-transfer coefficients. These advantages apply, in general, to any pair of fluid systems requiring heat exchange, when a suitable immiscible transfer fluid is chosen.

Until recently, little research had been undertaken on direct contact three-phase heat exchangers, in which one liquid undergoes phase change, while dispersed in another immiscible liquid. Requirements for economical water desalination units then motivated research into the basic mechanism of evaporation of a volatile liquid dispersed in an immiscible liquid, carried out by Sideman *et al.* [1–4], Klipstein [5] and Harriott and Wiegandt [6]. However, it is obvious that in its practical application the transfer agent must operate in a closed cycle, and provision must be made to recondense the vapors in a heat recovery system. Thus far, with the exception of several packed bed studies [7–9], and perforated exchangers [10], the only work reported on condensing vapor bubbles in an immiscible liquid was an heuristic preliminary study [11]. Therefore, a basic study of single bubbles is essential for the understanding and effective utilization of this important mode of heat transfer operation.

THEORETICAL

(a) *The model*

The collapsing bubble, as depicted in Fig. 1, is assumed to be spherical and rising freely in a vertical path. Alternatively, it can be envisioned as being at rest with the continuous medium moving against it with an approach velocity w_∞, which may be either constant or radius dependent.

As has been shown by a number of workers [2, 12–14), inviscid flow is a fairly valid assumption for freely rising bubbles. However, a collapsing bubble in a two-component system will tend to have a liquid–liquid interface.

Under this condition, internal circulation due to interfacial viscous effects, is considerably reduced, particularly when a monolayer film of condensed liquid is present on the wall. (Harkins [15] notes that the interfacial viscosity between water and a monolayer of normal chain alcohol is from 10^4 to 10^8 times larger than that of water itself.) The resulting surface viscosity may even arrest circulation, thereby forming, in effect, a rigid sphere. Visually, this effect is evident from a comparison between pictures taken of bubble collapse of single-component (pentane–pentane) and two-component (pentane–water) systems. Consistent with the obser-

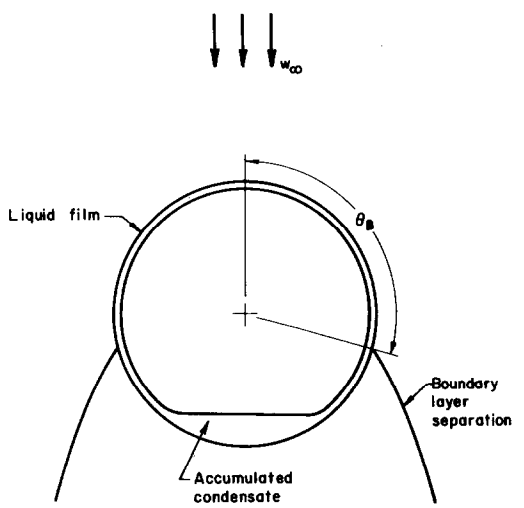

FIG. 1. Schematic of physical model.

vations of Bankoff and Mason [16] in a steam–water system, the surface of the pentane bubble in pentane liquid is highly irregular when compared to the smoother interface of the pentane bubble in water (Fig. 2, Ref. [11]). The former is typical of gas–liquid interfaces, while the latter behavior is more akin to liquid drops. Hence, the two-phase bubble will be treated here as a rigid sphere and a laminar flow field assumed for the continuous phase.

The process within the bubble is that of volatile vapors condensing upon a thin film that is assumed to be continuously draining toward the rear of the bubble, where the condensate is accumulated. For such a thin film, the outside heat transfer controls all but the final stages of bubble collapse (up to 95 per cent of the mass condensed). The actual heat transfer is assumed to occur at the interface of the bubble wall above the angle of separation of the boundary layer, denoted by θ_B. For small temperature differences (Jakob numbers <50) which are of interest for water-desalination schemes, the phenomenon treated here is heat transfer rather than liquid inertia controlled.

(b) *Method of solution*

A numerical solution for a laminar flow field around a rigid sphere was presented by Hamielec *et al.* [17]. However, a modification of such a solution for a contracting sphere would be highly untractable when coupled with the transient heat transfer problem which in itself requires a numerical solution. Hence, it is deemed advisable to derive expressions equivalent to the convective terms in the energy equation and circumvent the requirement for a solution for the laminar flow field. This is accomplished by introducing a velocity factor, k_V, dependent on the external fluid properties, and expressing the velocities in the energy equation in terms of the modified potential flow field. Griffith [18], was first to recommend the incorporation of a velocity factor into the equation for steady state heat transfer in potential flow in order to modify it for rapidly circulating drops. However, unlike his velocity factor defined as the ratio of true interfacial velocity and potential theory velocity, the velocity factor to be employed here is defined as that factor yielding potential convection terms equivalent to the actual laminar convection terms. The validity of such an approach has been demonstrated for the simple case of heat transfer in laminar flow over a flat plate [19].

The velocity factor is derived through relations with known solutions for steady state heat transfer to a sphere. Rearranging Froessling's

semiempirical relation [13] for the Nusselt number for steady state heat transfer to a rigid sphere yields

$$Nu = \frac{2}{\pi^{\frac{1}{2}}}(0{\cdot}25\, Pr^{-\frac{1}{3}} Pe)^{\frac{1}{2}} \tag{1}$$

whereas the Nusselt number for steady state heat transfer to a sphere in potential flow as evaluated by Boussinesq [12], is

$$Nu = \frac{2}{\pi^{\frac{1}{2}}} Pe^{\frac{1}{2}}. \tag{2}$$

Comparison between equations (1) and (2) gives

$$k_V = 0{\cdot}25\, Pr^{-\frac{1}{3}} \tag{3}$$

which represents the factor by which the potential flow solution is "transformed" to that of laminar flow around a sphere.

It must be emphasized that the implementation of this factor does not purport to specify the laminar flow field around the collapsing bubble, but rather to obtain the equivalent convective terms associated with the primary (translatory) flow. It is assumed the velocity factor derived from the above relationships for a sphere of constant radius can be applied for the case of a varying radius under study here.

(c) *The potential flow field*

In terms of the velocity potential ϕ, the axisymmetric flow must satisfy the Laplacian: $\nabla^2\phi = 0$ or

$$\frac{\partial}{\partial r}\left(r^2 \frac{\partial \phi}{\partial r}\right) + \frac{1}{\sin\theta}\frac{\partial}{\partial \theta}\left(\sin\theta \frac{\partial \phi}{\partial \theta}\right) = 0. \tag{4}$$

The boundary conditions are

$$\frac{\partial \phi}{\partial r} = w_\infty \cos\theta, \frac{\partial \phi}{\partial \theta} = -w_\infty r \sin\theta, r \to \infty \tag{5a}$$

$$\frac{\partial \phi}{\partial r} = -\dot{R}, \qquad r = R \tag{5b}$$

where w_∞ denotes the approach velocity. Boundary condition (5a) is satisfied by rectilinear flow around a sphere of constant radius. Denoting this flow with subscript s, we get

$$\phi_s = w_\infty \left(r + \frac{R^3}{2r^2}\right)\cos\theta. \tag{6}$$

This function yields a radial velocity that vanishes at $r = R$.

Boundary condition (5b) is satisfied by the equation for cavitational or sink flow [20]:

$$\phi_c = \frac{R^2\dot{R}}{r} \tag{7}$$

here denoted by the subscript c. This function generates a velocity field that vanishes at $r \to \infty$.

By superposition, the velocity field ls thus specified by

$$\phi = w_\infty \left(r + \frac{R^3}{2r^2}\right)\cos\theta + \frac{R^2\dot{R}}{r} \tag{8}$$

which in turn yields the accompanying stream function

$$\psi = \frac{w_\infty}{2}\left(r^2 - \frac{R^3}{r}\right)\sin^2\theta + R^2\dot{R}\cos\theta. \tag{9}$$

It is important to note that at high Péclét numbers the first terms (ϕ_s and ψ_s) in equations (8) and (9) represent the primary flow, while the second terms (ϕ_c and ψ_c) are associated with secondary flow.

(d) *The energy equation and boundary conditions*

The energy equation expressed in axisymmetric cylindrical coordinates is given by

$$\frac{\partial T}{\partial t} + u\frac{\partial T}{\partial \omega} + w\frac{\partial T}{\partial z} = \alpha\left[\frac{1}{\omega}\frac{\partial}{\partial \omega}\left(\omega\frac{\partial T}{\partial \omega}\right) + \frac{\partial^2 T}{\partial z^2}\right] \tag{10}$$

where z is the axis of symmetry; ω the circular radius; and w and u are, respectively, the velocity components in these directions.

Following Boussinesq, equation (10) in the

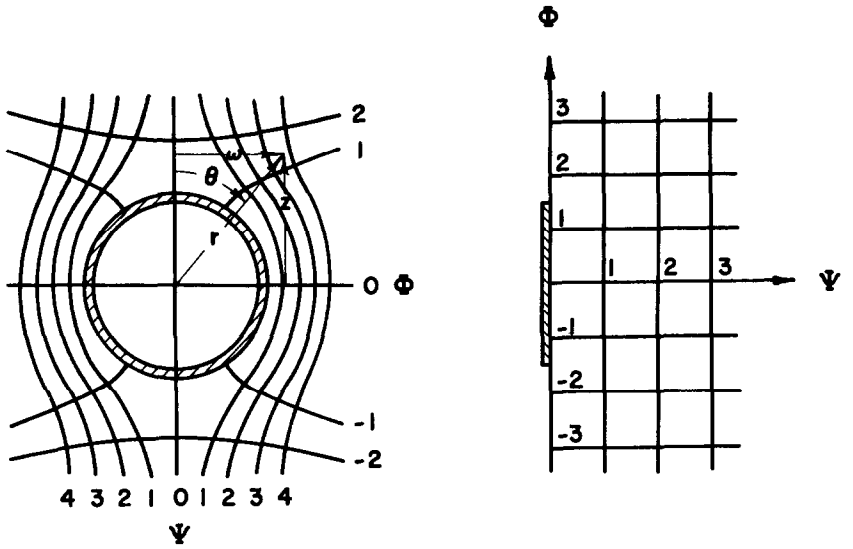

FIG. 2. Transformation of coordinates.

$\omega - z$ coordinates is transformed to the $\phi_s - \psi_s$ coordinate system (Fig. 2)

$$\frac{\partial T}{\partial t} = \alpha(u_s^2 + w_s^2)\left(\frac{\partial^2 T}{\partial \phi_s^2} + \omega^2 \frac{\partial^2 T}{\partial \psi_s^2}\right) + \left[\omega(u_c w_s - u_s w_c) - 2\alpha w_s - \frac{d\psi_s}{dt}\right]\frac{\partial T}{\partial \psi_s} + \left[u_s^2 + w_s^2 + u_c u_s - w_c w_s - \frac{d\phi_s}{dt}\right]\frac{\partial T}{\partial \phi_s} \quad (11)$$

where use is made of the following general relationships

$$u = -\frac{\partial \phi}{\partial \omega} = \frac{1}{\omega}\frac{\partial \psi}{\partial z} \quad (12a)$$

$$w = -\frac{\partial \phi}{\partial z} = -\frac{1}{\omega}\frac{\partial \psi}{\partial \omega}. \quad (12b)$$

We now define the following dimensionless parameters

$$\Theta \equiv \frac{T - T_\infty}{T^* - T_\infty}$$

$$\Phi \equiv \frac{\phi_s}{w_\infty R}, \qquad \Psi \equiv \frac{\psi_s}{w_\infty R^2}, \qquad \tau \equiv \frac{\alpha t}{R_o^2}$$

$$\beta \equiv R/R_o, \qquad \dot{\beta} \equiv \frac{d\beta}{d\tau},$$

$$y \equiv r/R, \qquad \mu \equiv \cos\theta$$

$$J \equiv \frac{u_s^2 + w_s^2}{w_\infty^2} = \left(1 - \frac{1}{y^3}\right)^2 + \frac{3}{y^3}\left(1 - \frac{1}{4y^3}\right)(1 - \mu^2)$$

$$Pe \equiv \frac{2R_o w_\infty}{\alpha}$$

where T^* is the saturation temperature of the vapor corresponding to the system pressure, p^*; T_∞ is the temperature at infinity, and R_0 is the initial radius. Introducing k_V, the final dimensionless form of the energy equation is

$$\frac{\partial \Theta}{\partial \tau} = \frac{J}{\beta^2}\left[\frac{\partial^2 \Theta}{\partial \Phi^2} + y^2(1 - \mu^2)\frac{\partial^2 \Theta}{\partial \Psi^2}\right] + \frac{1}{\beta}\left[k_V \frac{Pe}{2} J + \dot{\beta}\mu y\left(1 - \frac{1}{y^3}\right)^2\right]\frac{\partial \Theta}{\partial \Phi} + \left\{\frac{1}{\beta^2}\left[2\left(1 - \frac{1}{y^3}\right) + \frac{3}{y^3}(1 - \mu^2)\right] + \frac{\dot{\beta}}{\beta}(1 - \mu^2)\left(y^2 + \frac{1}{2y}\right)\left(1 - \frac{1}{y^3}\right)\right\}\frac{\partial \Theta}{\partial \Psi}. \quad (13)$$

Note that equation (13), the governing equation for the two-component bubble collapse, reduces to that of a single-component bubble collapse when $k_V = 1$.

For $Pe/2 \gg 1/(\beta k_V)$, the conduction in the ϕ_s (or Φ) direction is negligible in comparison with the convection. This implies that the ensuing solution is applicable to the (practical) range of comparatively high Péclét numbers (>1000). This assumption greatly facilitates the numerical computation required.

In dimensionless form in the $\Psi - \Phi$ coordinate system, the boundary conditions are:

$$\Theta(\Psi, \Phi, 0) = 0 \tag{14a}$$

$$\Theta(\Psi, \tfrac{3}{2}, \tau) = 0 \tag{14b}$$

$$\Theta(\infty, \Phi, \tau) = 0 \tag{14c}$$

$$\Theta(0, \Phi, \tau) = 0 \qquad \tfrac{3}{2} \geqslant \Phi \geqslant \Phi_B \tag{14d}$$

$$\frac{\partial \Theta}{\partial \Psi}(0, \Phi, \tau) = 0 \qquad \Phi_B > \Phi \geqslant -\frac{3}{2} \tag{14e}$$

where $\Phi_B = 1{\cdot}5 \cos \theta_B$. Boundary condition equation (14e) assumes that no heat transfer occurs at the bubble wall below the angle of boundary layer separation. This assumption is based on the fact that heat transfer in the wake of a rigid sphere in laminar flow is relatively insignificant [21].

(e) *Bubble temperature—effect of noncondensables*

The presence of noncondensables (usually air) within the bubble will reduce the partial pressure of the condensing vapors, resulting in a decrease in the corresponding saturation temperature. As the collapse proceeds, the effect of these noncondensables increases until condensation is halted, when the temperature difference between the bubble wall and the continuous phase decreases to zero.

For the normal range of bubble size encountered in this study (and in practice), surface tension effects on the pressure can be neglected. Hence, the pressure in the bubble is taken to correspond to that of the system, p^*, defined as the sum of the barometric and the average hydrostatic heads. For the low temperature differences, as employed in this study, Boyle's law is applicable for the noncondensable constituent within the bubble

$$p_g(V_T - V_L) = p_{g,f}(V_{T,f} - V_{L,f}) \tag{15}$$

where V_T refers to the total volume and the indices g, L and f denote the noncondensable, volatile liquid and final state, respectively. By a mass balance on the volatile liquid component:

$$\rho_v^* V_{T,0} \simeq \rho_{v,0} V_{T,0} = \rho_L V_L + \rho_{v,w}(V_T - V_L) \tag{16}$$

where $V_{T,0}$ is the initial total volume; and ρ_v^*, $\rho_{v,0}$ and $\rho_{v,w}$ denote the saturated vapor densities corresponding to T^*, $T_{w,0}$ and T_w, respectively.

Defining

$$G \equiv \rho_L/\rho_v \qquad G^* \equiv \rho_L/\rho_v^* \qquad G_w \equiv \rho_L/\rho_{v,w}$$

equation (16) yields

$$V_L = \frac{1}{G_w - 1}\left(\frac{G_w}{G^*} V_{T,0} - V_T\right) \tag{17}$$

which, when combined with equation (15), gives

$$\frac{p_g}{p_{g,f}} = \frac{\left(1 + \dfrac{1}{G_{w,f}}\right)\beta_f^3 - \dfrac{1}{G^*}}{\left(1 + \dfrac{1}{G_w}\right)\beta^3 - \dfrac{1}{G^*}} \tag{18}$$

where $\beta_f = R_f/R_0$. For systems whose operating pressure is low relative to the critical pressure, G is much larger than unity (about 200 for pentane), so that:

$$1 + \frac{1}{G} \simeq 1.$$

With $p_g = p^* - p_{v,w}$ and $p_{g,f} = p^* - p_{v,f}$ (where $p_{v,f} = p_{v,\infty}$), equation (18) reduces to

$$\frac{p^* - p_{v,w}}{p^* - p_{v,}} = \frac{\beta_f^3 - (1/G^*)}{\beta^3 - (1/G^*)}. \tag{19}$$

For the low temperature differences employed

here, a linear relationship suffices between temperature and pressure, and

$$\frac{p_{v,w} - p_{v,\infty}}{p^* - p_{v,\infty}} \simeq \frac{T_w - T_\infty}{T^* - T_\infty} \equiv \Theta_w \tag{20}$$

which, in combination with equation (19) yields

$$\Theta_w = \frac{\beta^3 - \beta_f^3}{\beta^3 - (1/G^*)}. \tag{21}$$

For a single-component, two-phase system, equation (21) reduces to [22]:

$$\Theta_w = \frac{\beta^3 - \beta_f^3}{\beta^3}. \tag{22}$$

The term $1/G^*$ in equation (21) is due to the condensed liquid, which accumulates in the bubble, in contrast to the single-component system, where the condensate merges with the continuous phase. In the absence of noncondensables, $\beta_f = G^{*-\frac{1}{3}}$ for two-component systems, and $\beta_f = 0$ for the single-component system. β_f for a typical bubble is obtained experimentally. In effect, Θ_w will vanish as β approaches β_f, thus halting the condensation process.

The relation for bubble temperature derived here, assumes a uniform distribution of noncondensables within the bubbles. However bubble collapse can induce a pile-up of noncondensables at the bubble wall, resulting in a simultaneous reduction in the wall temperature. To analyze this effect, a mathematical model incorporating mass convection and diffusion is required. Work along these lines is presently underway.

For better physical interpretation, a relationship between β_f and the initial concentration of the permanent gas within the bubble is presented. Starting with a bubble with an initial mole fraction, Γ, of noncondensables subjected to a system pressure, p^*, the initial pressure of the noncondensables, is given by the Gibbs–Dalton law, as

$$p_{g,0} = p^*\Gamma. \tag{23}$$

The final partial pressure of the noncondensables is given by

$$p_{g,f} = p^* - p_{v,\infty} \tag{24}$$

where $p_{v,\infty}$ is the vapor pressure corresponding to T_∞. Combining equation (23) and (24) yields

$$\frac{p_{g,0}}{p_{g,f}} = \frac{p^*}{p^* - p_{v,\infty}}. \tag{25}$$

For small temperature differences (as employed in this study) we introduce the simplified Clausius–Clapeyron equation given by

$$\frac{p^* - p_{v,\infty}}{p^*} = \frac{L\Delta T}{\hat{R}T^{*2}} \tag{26}$$

where $\hat{R}$ is the specific gas constant of the vapor. Substituting equation (26) into (25) gives

$$\frac{p_{g,0}}{p_{g,f}} = \frac{RT^{*2}}{L\Delta T}. \tag{27}$$

For the initial state where $\beta = 1$, equation (19) reduces to

$$\frac{p_{g,0}}{p_{g,f}} = \frac{\beta_f^3 - (1/G^*)}{1 - (1/G^*)} \simeq \beta_f^3 - \frac{1}{G^*} \tag{28}$$

since $G^* = \rho_L/\rho_V^* \gg 1$ (200 in our system). Substituting equation (27) into (28) yields the desired relationship

$$\beta_f = \left(\frac{\hat{R}T^{*2}}{L\Delta T}\Gamma + \frac{1}{G^*}\right). \tag{29}$$

Equation (29) shows that β_f depends on the concentration of noncondensables, as well as the temperature difference. Figure 3 depicts this dependency for a dispersed phase of pentane ($T^* = 309°K$) for various values of ΔT. For example, an initial mole fraction of noncondensables of $\Gamma = 0{\cdot}001$ in conjunction with a temperature difference of $\Delta T = 4°C$. yields a value of $\beta_f = 0{\cdot}235$. Obviously, the values of Γ

and ΔT necessary for collapse, have limits corresponding to an upper bound of $\beta_f = 1{\cdot}0$. The effect of noncondensables diminishes with a reduction of the ratio $\Gamma/\Delta T$. In the extreme case, when the ratio vanishes, a pure vapor bubble is obtained.

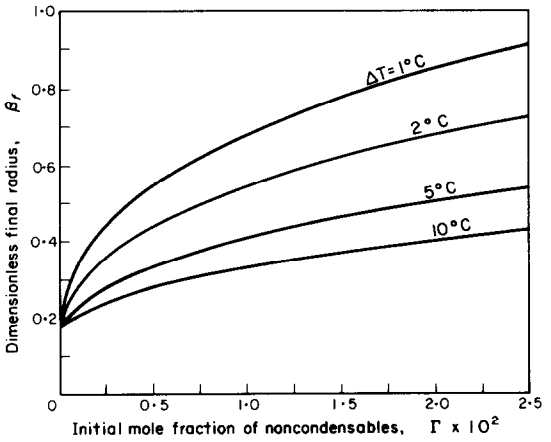

FIG. 3. Dimensionless final radius as a function of air concentration and temperature difference for dispersed phase of pentane at atmospheric pressure.

It is important to note that equation (29) is applicable only for a two-component system. For a single-component system, the analogous relation is given by

$$\beta_f = \left(\frac{\hat{R}T^{*2}}{L\Delta T}\right)^{\frac{1}{3}}. \tag{30}$$

When the ratio $\Gamma/\Delta T$, appearing in equation (30) vanishes, a pure vapor bubble is obtained, for which $\beta_f = 0$.

(f) *The collapse rate*

An energy balance at the wall yields

$$k\frac{\partial T}{\partial r} = \rho_{v,w} L\dot{R}, \qquad r = R \tag{31}$$

where L is the latent heat.

The translatory motion of the bubble causes the local heat transport at the wall to vary with the polar angle, θ. (This suggests that the collapse rate is not uniform over the bubble surface. However surface tension effects will tend to keep the bubble spherical-shaped.) Therefore, an integral relation at the wall is assumed:

$$4\pi R^2 \dot{R} L \rho_{v,w} = 2\pi k \int^{\theta_B} \left(\frac{\partial T}{\partial r}\right)_{r=R} \sin\theta \, d\theta \tag{32}$$

where the heat transfer area extends out to the separation angle of the boundary layer, θ_B. The collapse velocity is thus given by

$$\dot{R} = \frac{k}{2L\rho_{v,w}} \int_0^{\theta_B} \left(\frac{\partial T}{\partial r}\right)_{r=R} \sin\theta \, d\theta. \tag{33}$$

We now introduce a modified Jakob number, based on the external fluid properties, which are assumed constant, corresponding to T^*.

$$Ja \equiv \frac{\rho c_p (T^* - T_\infty)}{L\rho_v^*} = \frac{k\Delta T}{\alpha L \rho_v^*}. \tag{34}$$

In terms of the Boussinesq coordinates, equations (33) and (34) yield the collapse velocity in dimensionless form

$$\dot{\beta} = \frac{d\beta}{d\tau} = \frac{Ja}{2\beta}\frac{\rho_v^*}{\rho_{v,w}} \int_{\Phi_B}^{\frac{3}{2}} (1 - \tfrac{4}{9}\Phi^2) \times (\partial\Theta/\partial\Psi)_{\Psi=0} \, d\Phi. \tag{35}$$

(At the forward stagnation point, $\Phi = \frac{3}{2}$, $\Psi = 0$, the transformation is singular. This does not pose any difficulties in determining the temperature field, since the forward stagnation point constitutes part of the boundary. However, the singularity does preclude evaluation of the gradient at the bubble wall at this point, since equation (35) considers points on the boundary as being part of the temperature field. This hinderance can be circumvented by employing a Newton–Cotes open formula to numerically integrate equation (35). By this method, the end points are excluded from the calculation of the integral.)

The ratio $\rho_v^*/\rho_{v,w}$ which appears in equation

(35) is now obtained. By analogy to equation (20)

$$\Theta_w \simeq \frac{\rho_{v,w} - \rho_{v,\infty}}{\rho_v^* - \rho_{v,\infty}} = \frac{(1/G_w) - (1/G_\infty)}{(1/G^*) - (1/G_\infty)} \quad (36)$$

where, $G_\infty = \rho_L/\rho_{v,\infty}$ and ρ_L is assumed to be constant. Equation (36) yields

$$\frac{\rho_v^*}{\rho_{v,w}} = \frac{G_w}{G^*} = \frac{1}{\Theta_w - (G^*/G_\infty)(1 - \Theta_w)}. \quad (37)$$

Here, G^*/G_∞ is a given function of T^* and ΔT, and hence does not vary during the collapse.

Equations (13), (14), (20), (35) and (37) constitute the governing set of equations for bubble collapse in two-component systems. These were solved numerically to yield β and Nusselt number as functions of $\hat{\tau}$. Results are given after the presentation of the experimental portion of the study.

EXPERIMENTAL APPARATUS AND TECHNIQUE

The experimental set-up is schematically presented in Fig. 4. The glass column was 10 cm dia. surrounded by a square Perspex water jacket used for temperature control as well as to eliminate visual distortion within the column. The dispersed phase consisted of either pentane or isopentane bubbles; the continuous phase was either distilled water or aqueous-glycerol (70 per cent by volume). In order to ensure that the bubbles under study were completely vaporous when introduced into the test section of the apparatus, the bubble passed through a 7 cm layer of mercury maintained at a temperature above the boiling point of the volatile phase. The aqueous layer was 11 cm high. A revolving trap placed within the mercury layer over the injection port, enabled the bubbles to be introduced separately. The collapse of the single vapor bubbles emerging into the test section (the upper portion of the glass column) was photographed by a high-speed ciné-camera. Temperature measurements were obtained by means of thermocouples combined with differential thermometers.

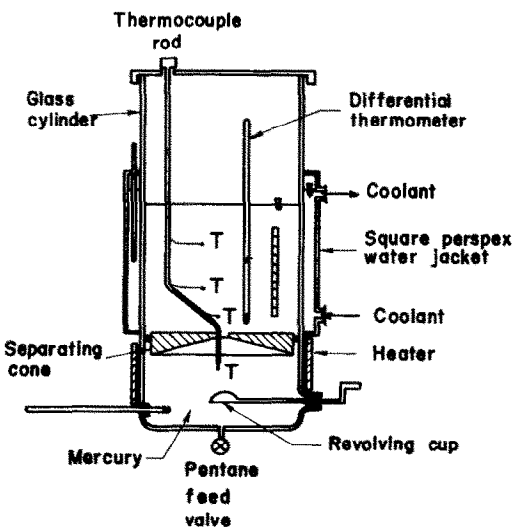

FIG. 4. Schematic of experimental apparatus.

The pertinent dimensions of the bubble were measured frame-by-frame. The measurements were then put into a data reduction computer program, which fit the data to exponential-decay type curves, by employing non-linear least squares techniques. The least squares residuals were weighted by calculations obtained from the standard deviation of the measurements. Using the fitted curves the computer program allowed time-dependent radius to be evaluated.

It was found that most bubbles collapsing in water exhibited a constant velocity of rise which varied for different bubbles from 170 to 250 mm/s. By contrast, the velocity of rise for each individual bubble collapsing in the aqueous-glycerol solution was not constant, showing a monotonic decrease during the collapse. The overall velocity range obtained for bubbles in this viscous medium was 30–300 mm/sec.

RESULTS AND DISCUSSION

In order to present results in a meaningful manner, the Péclét number for the system will be defined. The velocity of rise, w_∞^*, will be taken as that corresponding to half the initial bubble volume, or $\beta^3 = \frac{1}{2}$. On this basis, the

Péclét number is designated as

$$Pe^* = (2R_0 w_\infty^*)/\alpha.$$

The dimensionless time, appropriate for bubble collapse with translatory motion, is [3]

$$\hat{\tau} = Pe^{*\frac{1}{2}} Ja\, \tau.$$

Out of the 200 bubbles photographed, some twenty bubbles randomly selected to represent the three systems employed, were analyzed.

Graphical comparisons between experimental and theoretical bubble collapse are shown in Figs. 5 and 6, in terms of the β–$\hat{\tau}$ coordinates. As seen in Fig. 5, the agreement between experiment and theory for the runs in water is especially good, indicating the applicability of the theory to these practical systems for all the bubble sizes ($1{\cdot}5 < R_0 < 5$ mm). Generally, good agreement between experiment and theory was noted for runs in aqueous-glycerol, in small bubbles ($R_0 < 2{\cdot}3$ mm). However the larger bubble (shown in Fig. 6) in this system, exhibit experimental collapse rates that are markedly faster than the corresponding theoretical collapse

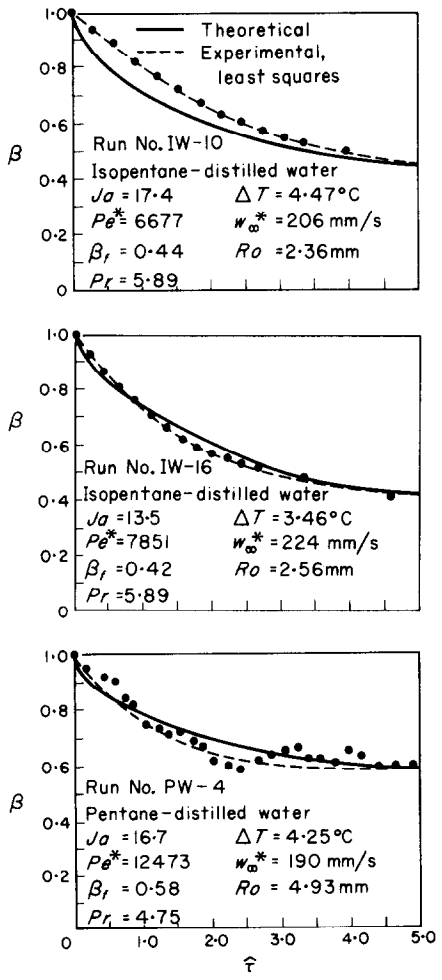

FIG. 5. Comparison between experiment and theory for the isopentane–distilled water and pentane–distilled water systems.

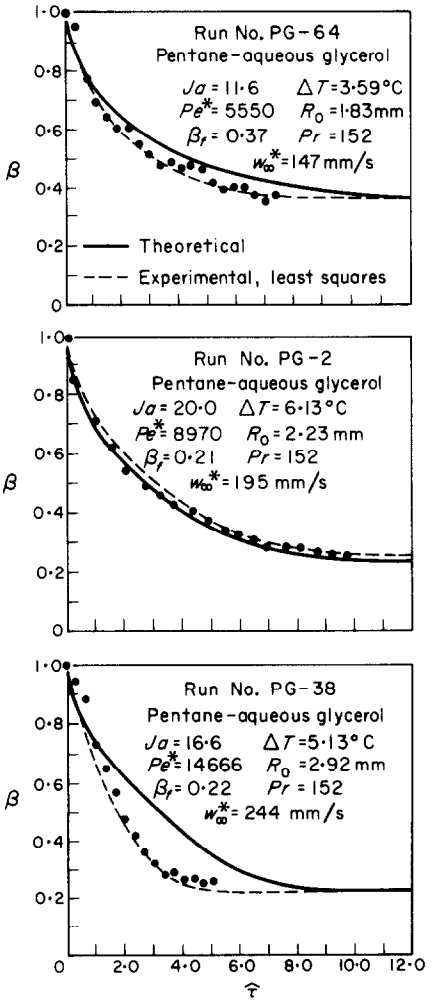

FIG. 6. Comparison between experiment and theory for the pentane–aqueous glycerol system.

rates. This indicates that the more viscous aqueous-glycerol induces circulation within the larger bubbles. This is manifested in two ways; the velocity factor, k_V, is increased toward the value of unity representing potential flow; the angle of boundary-layer separation increases, shifting toward the rear, beyond the value of $\theta_B = 100°$ for rigid spheres, used in the theoretical calculation. For potential flow, no separation will occur and θ_B is equal to 180°.

Theoretical β–$\hat{\tau}$ curves, calculated by the finite difference method, are presented in Figs. 7 and 8, showing the effect of Jakob and Péclét numbers on bubble collapse. In generating these curves, w_∞ was assumed constant for each bubble; hence, $Pe^* = Pe$. The value of the velocity factor ($k_V = 0{\cdot}149$) was taken to correspond to a continuous medium of water at the normal boiling temperature of pentane. Note that by the definition of $\hat{\tau}$, the abscissa in Figs. 7 and 8 contains the Pe and Ja numbers, which tends to obscure the physical interpretation of the results. However, this presentation is advantageous as it allows comparison with an approxi-

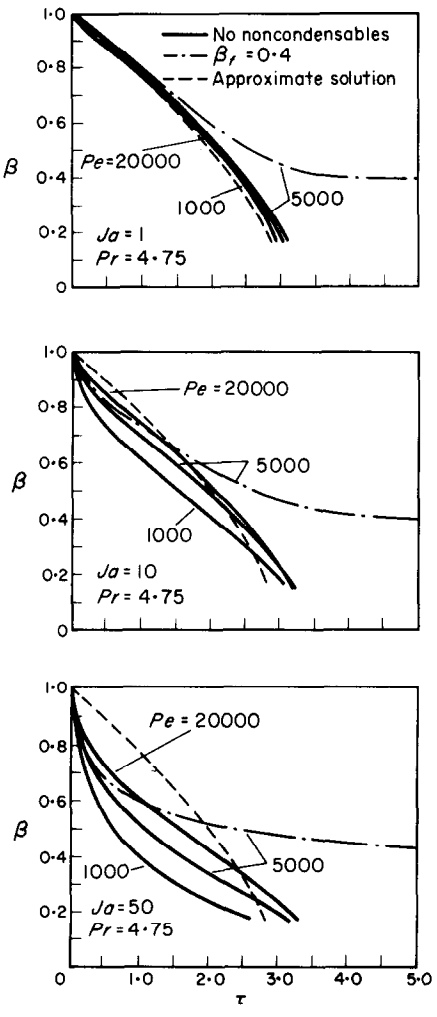

FIG. 7. Effect of Péclét number on bubble collapse.

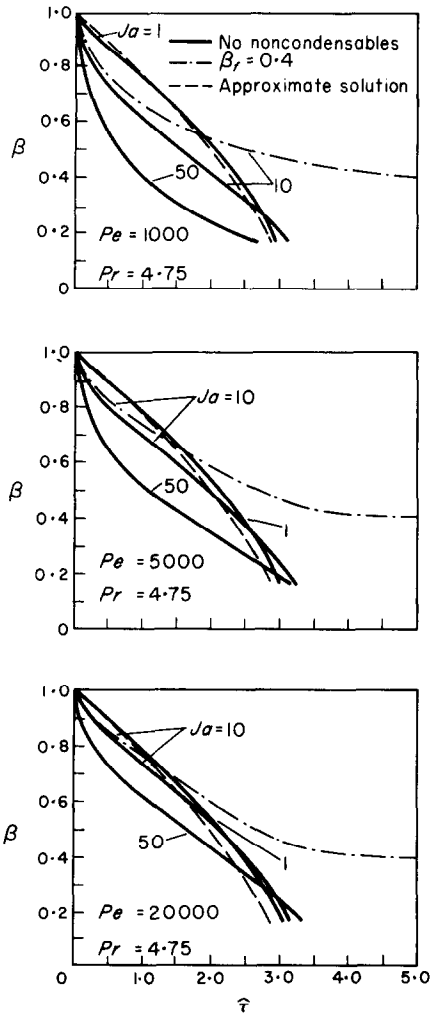

FIG. 8. Effect of Jakob number on bubble collapse.

mate analytical solution for bubble collapse in the absence of noncondensables, also included in these figures. This solution is obtained in a manner analogous to the analytical treatment of bubble collapse in single-component systems [19]. Briefly, this is accomplished by assuming quasi-steady state heat transfer along with potential flow around the sphere with an approach velocity of $k_V w_\infty$, which yields:

$$\beta = \left(1 - \frac{3}{2}\frac{k_v^{\frac{1}{2}}}{\pi^{\frac{1}{2}}}\hat{\tau}\right)^{\frac{2}{3}}. \quad (38)$$

For $k_V = 1$, equation (38) reduces to the approximate solution for single component systems [19].

Also included in Figs. 7 and 8 is a curve representing a typical solution for collapse in the presence of noncondensables. The effect of Péclét parameter on bubble collapse is shown in Fig. 7, indicating that bubble collapse is faster at higher Pe numbers which represent higher convection rates and thinner thermal boundary layers. The proximity and/or similarity of the shape of the finite difference curves to the analytical—albeit approximate—quasi-steady state solution indicates that at high Pe numbers, the heat transfer regime is fairly close to steady state.

In general, bubble collapse consists of two stages of heat transfer. The first stage is a transient mode where the thermal boundary layer is developing. This stage manifests itself by a decrease in the collapse rate. The second stage is characterized by steady-state heat transfer, i.e. a constant heat flux at the wall. For this period, the curves show a monotonically increasing collapse rate, corresponding to the increasing ratio of interfacial surface area to bubble volume. In accordance with these observations, large Péclét numbers increase the dominance of the second stage on bubble collapse, as seen, for example, in Fig. 7 for $Pe = 20000$. By contrast, the curve representing $Pe = 1000$ shows the first stage to dominate a large part of the collapse process.

Figure 8 shows the effect of the Jakob number on bubble collapse. As is to be expected, bubble collapse is slower at lower Ja numbers, which may be taken to represent smaller temperature differences.

It is evident that for a given system, the effect of increasing the Ja number corresponds to an increase in ΔT; hence to a thickening of the thermal boundary layer. Conversely, low Ja numbers imply thin thermal boundary layers. and a tendency to attain steady-state in a relatively short period of time. The curve for $Ja = 1$ shows that steady-state dominated bubble collapse produced by the correspondingly low ΔT. By contrast, the curve representing $Ja = 50$ indicates a dominant period of transient heat transfer due to the thick thermal boundary layer, corresponding to large ΔT. This effect will be amplified at low Pe number, say 1000, coupled with $Ja = 50$, which will result in an extremely thick boundary layer. This coupling demonstrates the interrelated effect of these two parameters on the collapse rate. A low Pe or high Ja number yields a relatively large period of transient heat transfer, while a high Pe or low Ja number results in a dominant period of steady-state heat transfer.

The presence of noncondensables lowers the vapor pressure and, hence, the saturation temperature of the vapor. As the vapor condenses,

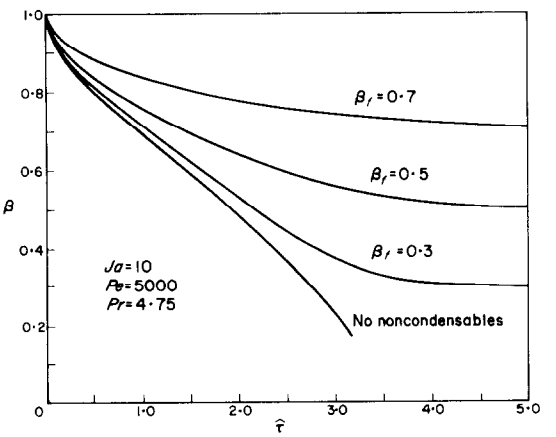

FIG. 9. Effect of final dimensionless radius on bubble collapse.

this effect becomes increasingly pronounced until collapse is arrested, when the saturation temperature decreases to a value equal to the approach temperature, T_∞, of the external phase. Thus, the extent of collapse is also affected by the temperature difference employed in the system.

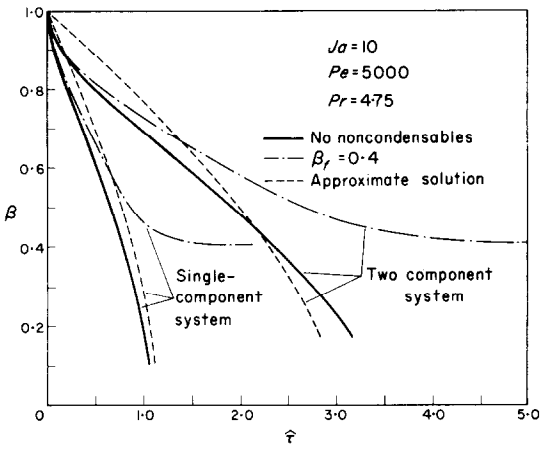

FIG. 10. Comparison between bubble collapse of single- and two-component systems.

In the analytical treatment of bubble collapse, the presence of noncondensables was accounted for, in terms of β_f, the final dimensionless radius. Figure 9 shows the effect of noncondensables on the collapse rate for a two-component system for values of β_f ranging from 0·7 down to $1/G^{*\frac{1}{3}}$, the lower value being appropriated for a pure vapor bubble. As seen, collapse is halted when β decreases to a value equal to β_f. Higher values of β_f signify a more pronounced effect of noncondensables resulting in reduced collapse rates.

A comparison between single (pentane) and two-component (pentane–water) systems is depicted in Fig. 10, for a typical set of Pe and Ja numbers. It is evident that in terms of the dimensionless $\beta - \hat{\tau}$ coordinates, bubble collapse is faster for the single-component system. This is as expected since the single-component system is in pure potential flow, whereas the two-component system has an immobile bubble wall. However, for a given initial bubble size, and given identical temperature differences and velocities of rise for the two systems, the physically measured rate of collapse, $\dot{R}$, may be faster in the two-component system than that obtained in the corresponding single component system. This is due to differences in external fluid properties. Thus, for example, with identical initial radius, temperature differences and velocities of rise, pentane bubbles collapse in water approximately 50 per cent faster than pentane bubbles collapsing in pentane.

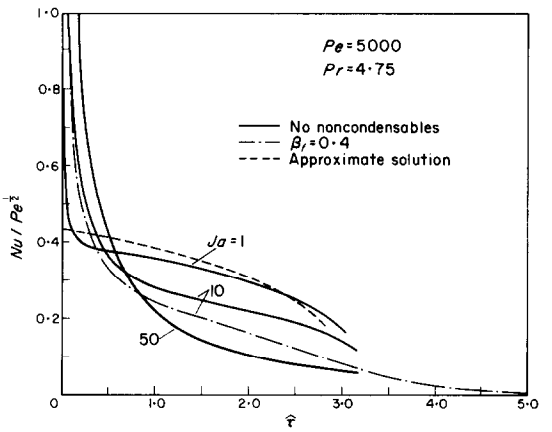

FIG. 11. Representative theoretical curves for the time-dependent Nusselt number.

Representative theoretical curves for the time dependant Nusselt number, defined as

$$Nu \equiv \frac{h2R}{k} = \frac{q}{A\Delta T}\frac{2R}{k} \tag{39}$$

are given in Fig. 11, for various values of the Jakob number. As it is to be expected, high Pe or Ja numbers yield high heat transfer rates.

REFERENCES

1. S. SIDEMAN and G. HIRSCH, *Israel J. Tech.* **2**(2), 234 (1964).
2. S. SIDEMAN, G. HIRSCH and Y. GAT, *A.I.Ch.E. Jl* **11**(6), 1019 (1965).
3. S. SIDEMAN and J. ISENBERG, *Desalination* **2**, 207–214 (1967).

4. S. SIDEMAN and Y. TAITEL, *Int. J. Heat Mass Transfer* 7, 1273 (1964).
5. D. KLIPSTEIN. D.Sc. Thesis, M.I.T., Cambridge, Mass. (1963).
6. P. HARRIOTT and H. WIEGANDT, *A.I.Ch.E. Jl* **10**(5), 755 (1964).
7. V. C. RAI and K. L. PINDER, *Can. J. Chem. Engng* **45**, 170 (1967).
8. C. R. WILKE, C. T. CHENG and J. W. WESTATER, *A.I.Ch.E. Jl* 7(4), 578 (1961).
9. T. K. SHERWOOD and F. A. L. HOLLOWAY, *Trans. A.I.Ch.E.* **36**, 39 (1940).
10. P. T. WALKER, I. NEWSON and K. D. B. JOHNSON, *Desalination* **2**, 196–206 (1967).
11. S. SIDEMAN and G. HIRSCH, *A.I.Ch.E. Jl* **11**(6), 1019 (1965).
12. M. J. BOUSSINESQ, *J. Math. Pures Appl.* Ser. 6, **1**, 310 (1905).
13. V. G. LEVICH, *Physiochemical Hydrodynamics*. Prentice-Hall, New Jersey (1962).
14. E. RUCKENSTEIN, *Chem. Engng Sci.* **10**, 22–30 (1959).
15. W. D. HARKINS, *The Physical Chemistry of Surface Films*. Reinhold, New York (1952).
16. S. G. BANKOFF and J. P. MASON, *A.I.Ch.E. Jl* **8**(1), 30 (1962).
17. A. E. HAMIELEC, T. W. HOFFMAN and L. L. ROSS, *A.I.Ch.E. Jl* **13**(2), 212 (1967).
18. R. M. GRIFFITH, *Chem. Engng Sci.* **12** 198–213 (1960).
19. J. ISENBERG, D.Sc. Thesis, Technion—Israel Inst. Tech., Haifa, Israel (1969).
20. L. M. MILNE-THOMSON, *Theoretical Hydrodynamics*, 5th ed. Macmillan, London (1968).
21. K. LEE and H. BARROW, *Int. J. Heat Mass Transfer* **11**, 1013–1026 (1968).
22. D. D. WITTKE and B. T. CHAO, *J. Heat Transfer* **89**, 17–24 (1967).

TRANSPORT DE CHALEUR PAR CONTACT DIRECT AVEC CHANGEMENT DE PHASE: CONDENSATION DE BULLES DANS DES LIQUIDES NON-MISCIBLES

Résumé—La condensation de bulles dans des liquides non-miscibles est associée au développement d'échangeurs de chaleur à trois phases applicables à la résupération de la chaleur pour de faibles forces d'entraînement.

Des bulles isolées de fluides organiques volatils se dégonflant sous des conditions contrôlées de transport de chaleur lorsqu'elles montent librement dans de l'eau et des solutions aqueuses de glycérol ont été étudiées expérimentalement et théoriquement. A la différence de la condensation dans des systèmes à constituant unique, le système à trois phases et à deux constituants est caractérisé par l'accumulation de condensat au voisinage de la bulle qui se dégonfle, ce qui empêche grandement la mobilité interfaciale. Une solution par différences finies dans le champ de l'écoulement laminaire a été obtenue en modifiant le champ de l'écoulement potentiel pour fournir des termes de convection équivalents aux termes laminaires dans l'équation de l'énergie. On a tenu compte également de la présence de gaz non-condensables. L'accord avec l'expérience est trés bon, particulièrement à de faibles nombres de Jacob.

WÄRMEÜBERGANG MIT PHASENÄNDERUNG: TROPFENKONDENSATION IN UNMISCHBAREN FLÜSSIGKEITEN

Zusammenfassung—Die Kondensation von Blasen in einer mit dem Blasenkondensat unmischbaren Flüssigkeit hängt mit der Entwicklung von Drei-Phasen-Wärmetauschern zusammen, die zur Wärmegewinnung bei kleineren Temperaturgefällen dienen.

Einzelne Blasen von flüchtigen organischen Stoffen, die beim Aufsteigen in Wasser oder in einer Wasser-Glycerin-Lösung kondensieren, wurden experimentell und theoretisch untersucht. Die Kondensationsgeschwindigkeit wird dabei von der Wärmeabfuhr bestimmt. Im Gegensatz zur Kondensation in Ein-Komponenten-Systemen wird das Zwei-Komponenten-, Drei-Phasensystem charakterisiert durch eine Akkumulation von Kondensat innerhalb der kondensierenden Blase, wodurch die Beweglichkeit der Grenzfläche stark vermindert wird. Mit Hilfe eines Differenzenverfahrens wurde eine Lösung im laminaren Strömungsbereich ermittelt, indem die Potentialströmung in der Weise abgewandelt wurde, dass konvektive Glieder ähnlich den laminaren Gliedern in der Energiegleichung erhalten werden. Die Anwesenheit von unkondensierbaren Gasen wurde berücksichtigt. Die Übereinstimmung mit dem Experiment ist, besonders bei niedrigen Jakobzahlen, sehr gut.

ПРЯМОЙ КОНТАКТНЫЙ ТЕПЛООБМЕН ПРИ ФАЗОВОМ ИЗМЕНЕНИИ. КОНДЕНСАЦИЯ ПУЗЫРЬКОВ В НЕСМЕШИВАЮЩИХСЯ ЖИДКОСТЯХ

Аннотация—Исследование конденсации пузырьков в несмешивающихся жидкостях связано с разработкой трехфазных теплообменников, применяемых для регенерации тепла при небольших движущих силах.

Экспериментально и теоретически исследовались единичные пузырьки летучих органических жидкостей, конденсирующихся в условиях, контролируемых переносом тепла во время свободного подъема в воде и водно-глицериновых растворах. В противоположность конденсации в однокомпонентных системах, двухкомпонентная трехфазная система характеризуется накоплением конденсата в пределах конденсирующегося пузырька, что значительно уменьшает подвижность поверхности раздела. Получено решение в конечных разностях в поле ламинарного течения путем изменения поля потенциального течения для получения конвективных членов, эквивалентных ламинарным членам в уравнении энергии. Учитывается также наличие неконденсируемых пузырьков. Получено хорошее согласование с экспериментом, в особенности при малом значении числа Якоба.